

Analysis of Al-Si Layer on Steel Sheet during Thermo Mechanical Processing Using Microscopic Methods

Sylvia Kusmierczak, Michal Slavik

Faculty of Mechanical Engineering, J. E. Purkyne University in Usti nad Labem. Pasteurova 3334/7, 400 96 Usti nad Labem. Czech Republic. E-mail: sylvia.kusmierczak@ujep.cz

High strength steel 22MnB5 according to DIN EN 10083-3 belongs to the group of HF steels frequently used in the production of coachwork. Using the thermo mechanical pressing can be achieved that these steels have strength of about 1500 MPa. The surface of this steel is provided with a protective coating to protect it from oxidation. Galvanic ally, a Zn-based layer is used to provide cathodic protection. The Zn-based layer is limited by the temperature which is insufficient for TMP. Hot-dip galvanizing is also applied to an Al-based layer that does not serve as a cathodic protection but is used as an effective oxidation barrier. The quality of the Al-Si layer is important with regard to the resulting quality of the formed blank. The properties of the surface Al-Si layer affect not only the conditions for their application to the steel blank but also the external conditions which are determined by the conditions of the thermo-mechanical processing into the shape of the finished product. To assess the properties of this layer, microscopy methods, namely light and electron microscopy, were used. On the basis of analyzes, conclusions were drawn that should lead to securing the Al-Si layer with the required properties.

Keywords: Light Microscopy, electron Microscopy, Al-Si Layer, Properties

1 Introduction

The automotive industry is one of the most important manufacturing industries. In the Czech Republic, the automotive industry is constantly developing, increasing its production volume, increasing its share of industrial production. The automotive industry does not only include the assembly of vehicles that are supplied to consumers, but also the production of individual car parts, starting with car body parts, body parts, electronics or, for example, engines parts. Under the automotive industry, dozens of subcontractors, quality control, and the complex logistical and technological processes that arise in this sophisticated chain of dependent activities are also required.

Automotive steels are complex materials with thoroughly selected chemical compositions and multiphase structures from tightly controlled heat and cooling processes. The various mechanisms for improving all property values (mechanical properties, elongation, degree of stiffness) are designed to meet the very stringent safety requirements of today's vehicles, reducing their weight and produced emissions, all at an acceptable production cost. These steels are also known as the AHSS Advanced High-Strength Steel, advanced high-strength steel, which is the current conventional steels differ primarily in the microstructure. Conventional HSS steels are single-phase. AHSS steel has a microstructure mainly containing martensite, bainite, austenite or residual austenite in such an amount that unique mechanical properties can be created [1].

Steel with the trade name USIBOR 1500 or 22MnB5 according to DIN EN 10083-3 belonging to the group of HF steels. The pressing process has the following main steps:

- Heating to a temperature $(30 \div 50)^\circ\text{C}$ above the temperature curve A_{c3}
- A homogeneous austenitic microstructure is obtained from the ferritic-perlite structure

- when handling from a furnace to a mold, the sheet itself without the surface layer would be subjected to strong oxidation and decarburization, therefore a protective Al-Si or Zn layer
- forming the sheet takes place in one step, simultaneously with its cooling in a form where the martensitic structure of the sheet [2-5].

In the case of steels for thermo mechanical processing, the zinc-based surface layer is limited by the processing temperature. Hot-dip galvanizing is also applied to an Al-based layer which does not serve as a cathodic protection, since it has a similar electrochemical potential but provides an effective barrier to protect the surface from oxidation. The Al-Si layer increases the resistance of the material and does not impair its refractoriness.

The Al-Si layer (AlSi10F3) is applied at 675°C to the etched surface of 22MnB5 steel at various thicknesses, most often $(25-35)\mu\text{m}$. The layer of AlSi10Fe3, after application to steel, is composed of two layers, the top layer contains the eutectic two-phase Si anchored in the Al matrix and the thin layer below it is composed of intermetallic phases of the type Al8Fe2Si and Al5Fe2. The irregular shape of the Al8Fe2Si phase is the result of diffusion of Fe into the liquid Al-Si layer during deposition of the surface layer where Al8Fe2Si solidifies at the interface of the layers. Later diffusion of Fe into the phase formed by Al8Fe2Si promotes the formation of Fe-enriched phase of Al5Fe2 type. Between these two phases, Al2Si3Fe3 precipitates are also formed. The entire surface layer after application with reference to the individual phases is shown in Fig. 1 and 2 [6].

In Fig. 1 it is possible to see the interface of the surface layer AlSi10Fe3 and the steel 22MnB5, which contains several transition layers. The total thickness of AlSi10Fe3 is $30\mu\text{m}$. After hot pressing (conditions: $T_{\text{AUS}} = 920^\circ\text{C}$, $t_{\text{AUS}} = 6\text{ min}$, cooled in the tool) it is characterized by a

martensitic microstructure 22MnB5 addition ($10 \div 12$) micron thin layer of Al-Si enriched Fe_α incurred during the diffusion of Al at austenitizing 22MnB5. Direct correlation shows that the more diffuse the Al into the steel, the Al-Si layer enriched Fe_α stable on cooling and does not change to martensite. AlSi10Fe3 is characterized by the fact that fragile intermetallic phases of the Al_xFe_y type ($\text{Al}_{13}\text{Fe}_4$, Al_5Fe_2 , Al_2Fe and AlFe) are generated, and the most important ones are shown in Fig. 2. In the surface layer there is a particularly fragile intermetallic phase Al_5Fe_2 , which has low fracture toughness ($1 \text{ MPa}\cdot\text{m}^{1/2}$). The formation of brittle intermetallic phases promotes the initiation and propagation of cracks during forming [6-8, 11].

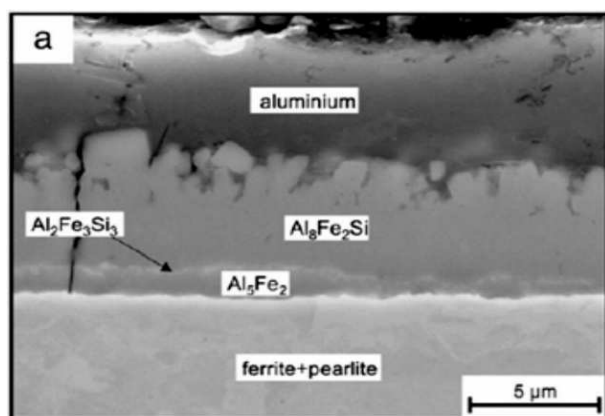


Fig. 1 The interface between 22MnB5 and AlSi10Fe3 after thermal spraying [6]

It should be borne in mind that cracks may vary depending on the region formed [9, 10], especially in sheets that are formed comprehensively. An example is a study

Tab. 1 Chemical composition 22MnB5 according to DIN EN 10083-3 [wt. %]

C	Si	Mn	Cr	Mo	P	S	Ti	Al	B
< 0.25	0.15 - 0.40	< 1.40	≤ 0.5	≤ 0.35	≤ 0.03	≤ 0.01	< 0.1	< 0.1	0.001 - 0.005

The delivered product was free of oil protection, so it is necessary to use the Al-Si layer during production to provide the necessary corrosion resistance in handling before the forming process itself. Requirements for the chemical composition of AS150 surface Al-Si layer are shown in Table 2.

Tab. 2 Requirements on the chemical composition of the surface layer of an Al-Si of AS150

Element [wt. %]	Al	Si	Fe
min.	80	5	-
max.	95	15	4

The thickness of the surface Al-Si layer is determined according to BS EN 10346: 2009. A typical thickness range is in the range ($19 \div 33$) μm .

Sheet metal processing technology: the temperature achieved in the furnace is 950°C , the time of the sheet remains in the furnace in the range (300 to 900) s. Thereafter, the work piece is molded, the pressing temperature is approximately 830°C . Cooling time in the form: 8 seconds. Then the part is moved to a strip where it is cooled

[7] which dealt with the cracks in different areas of the formed sheet and at different distances of clearance between the upper and lower molds during pressing.

The aim of the article is to point out the usage of microscopy methods in the analysis of surface Al-Si surface properties on steel sheet during surface forming.

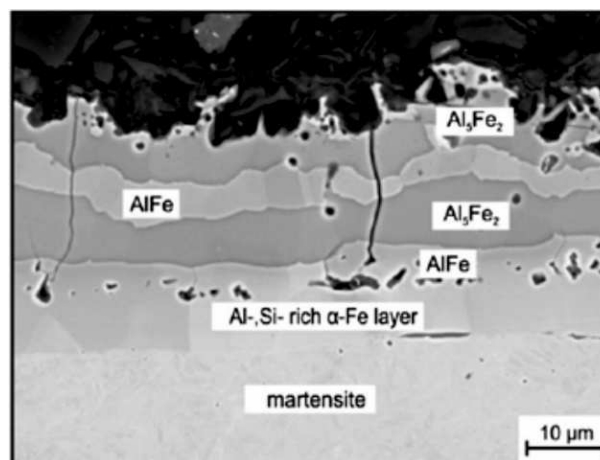


Fig. 2 Interface between 22MnB5 and AlSi10Fe3 after hot pressing [6]

2 Description of the situation

The material of the blank sheet before pressing is distributed under the trade name Usibor 1500 ALUs, which is called material 22MnB5 according to DIN EN 10083-3. The microstructure of the material is ferritic-pearlitic with the Al-Si layer labelled under the trade name AS150. The chemical composition of the 22MnB5 steel according to the certificate is shown in Tab. 1. Thickness of the sheet is 1.8 mm.

down to 100°C .

3 Analysis of the Al-Si layer

The surface layer of the analyzed part was analyzed before and after hot forming of the sheet. The equipment that was used was the Tescan Vega 3 electron microscope and the Olympus BX51M optical microscope.

At first were samples analyzed which showed degradation of the protective layer. Impaired surface layer is always located on the oblique surface of the molding. In practice, this kind of degradation is called "galling". On samples 1 and 2 (Figures 3 and 4) it is visible that the surface layer is traced to the corners of the damaged area. Regular macro cracks can also be seen on the images, especially in areas where the surface layer is not damaged. The macro cracks are in a regular spacing ($150 \div 180$) μm with a width of $30 \mu\text{m}$, Fig. 3. Their formation is due to insufficient compression in the mold, due to poor or no contact with the sheet, it cools down at a lower velocity and in the base material there are tensile stresses cooler surface layer, cause macro cracks. To the forma-

tion of macro cracks contributes Kirkendall effect that assesses the chemical potentials of the various elements, in this case is most likely a Fe - base material and Fe_2Al_5 dominant phase, which is represented by the most resources. The principle of this phenomenon is the formation of a vacancy mechanism, in which atoms from a certain thickness of the surface Al-Si layer are transferred to a lower thickness of the surface layer.

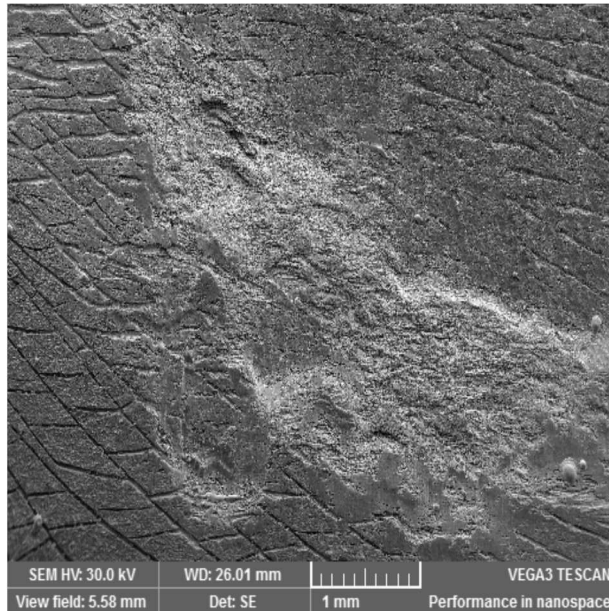


Fig. 3 Sample 1, damaged surface

Tab. 3 Point EDX analysis of spherical inclusion 1 [wt.%]

Element	Content	Element	Content	Element	Content	Element	Content
Fe	51.97	Mo	6.76	Na	0.39	P	0.20
O	27.92	Nb	3.08	Mg	0.30	Ti	0.10
Mn	8.14	Al	0.74	Bi	0.29	V	0.03

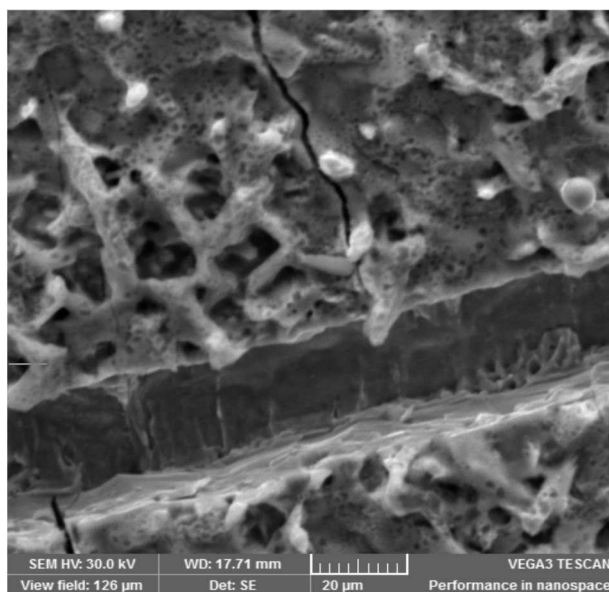


Fig. 5 Sample 1, cracks from the surface to the base material

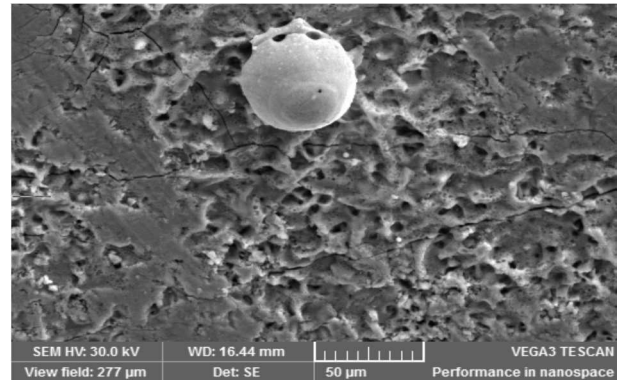


Fig. 4 Sample 1, spherical inclusion 1, detail

For more detailed analyzes of the state of the surface layer was observed in the presence of spherical inclusions (Fig. 3, 4). The results of EDX analysis of spherical inclusion 1 (Table 3) indicate that this is the inclusion on the base of iron oxides

The Nb and V elements are not defined in the chemical composition of the base material (22MnB5 steel) or the surface Al-Si layer. For this reason, it can be assumed that these are elements that include the forming tool. The Nb content, together with Ti and V, provides steel precipitation, grain refinement, and these elements can also influence the temperature of the polymorphic transformation ferrite ↔ austenite.

In the surface layer there is often a uniform and regular repetition cracks of the surface layer to the base material. In this part of the surface there are also spherical inclusions, Fig. 5.

Sample 2 shows the state of the surface of the sheet material, where there is no significant plastic deformation of the surface layer (Fig. 6).

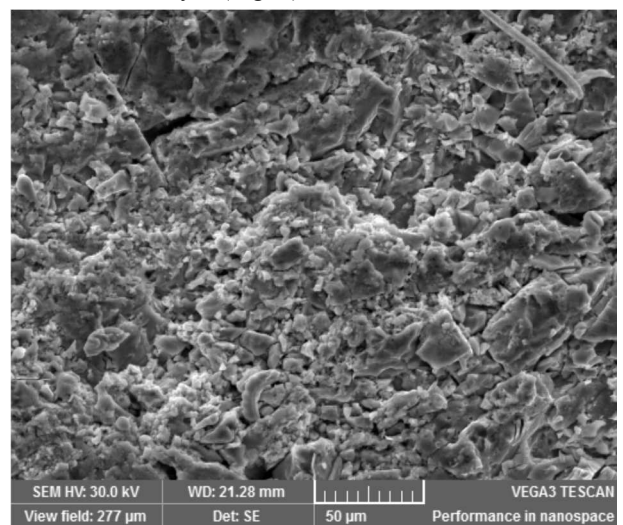


Fig. 6 Sample 2, condition of the surface layer

For other samples (samples 3 and 4), the surface layer was discontinued and the diffusion layer was observed. The samples were metallographically prepared and etched by Nital (3% HNO_3).

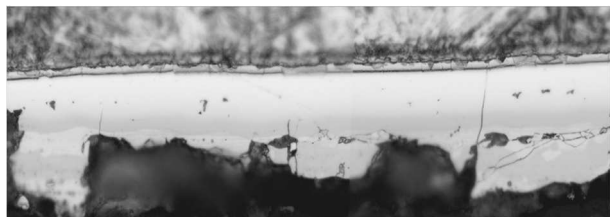


Fig. 7 Sample 3, bottom surface layer, mag. 500x

According to the standards, the stable surface layer should have a thickness $(30 \div 50) \mu\text{m}$ and the thickness of the diffusion layer should be less than $16 \mu\text{m}$. The section of the surface layer are shown in Fig. 7 shows different bands resulting from heat treatment and diffusion processes Fe to Al Si layer. In the surface layer there are cavities which endanger the stability of the surface layer. The surface layer also contains micro cracks that are a natural phenomenon in this surface treatment. From the observation of the state of the surface layer, it can be seen that none of the values correspond to the requirements for the prescribed thickness to what extent the thickness of the layer is uneven, unstable, non-constant, Fig. 8 a 9.

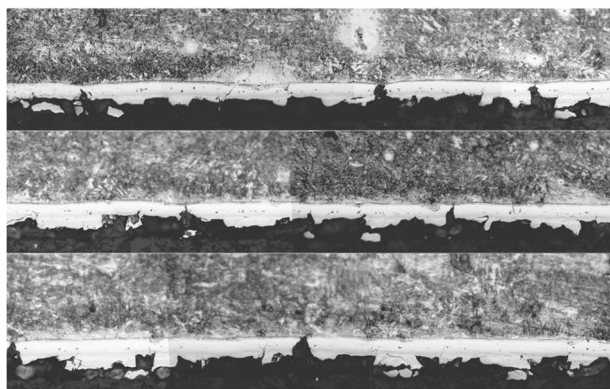


Fig. 8 Sample 4, underside of the surface layer, mag. 200x

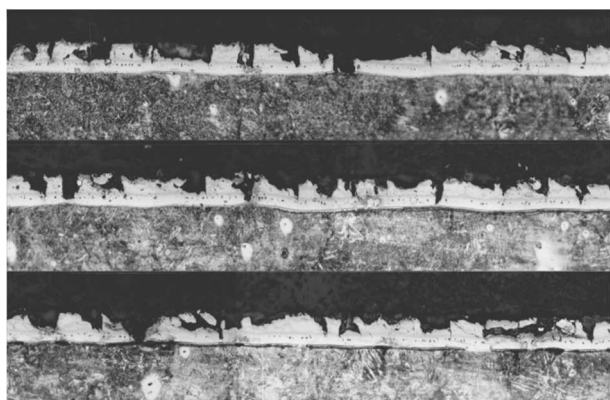


Fig. 9 Sample 4, top side of the surface layer, mag. 200x

The macro cracks are seen but are not of the same type as for sample 1. These macro cracks are wedge shaped. In the previous case, it was a flat, periodically repeating

and equally deep damage to the surface layer. In some places, the surface layer was completely removed and consequently the corrosion resistance of the sheet was deteriorated. In those places where there is no surface layer, a corrosion microcell may occur which causes pitting corrosion attack between the base material and the protective layer.

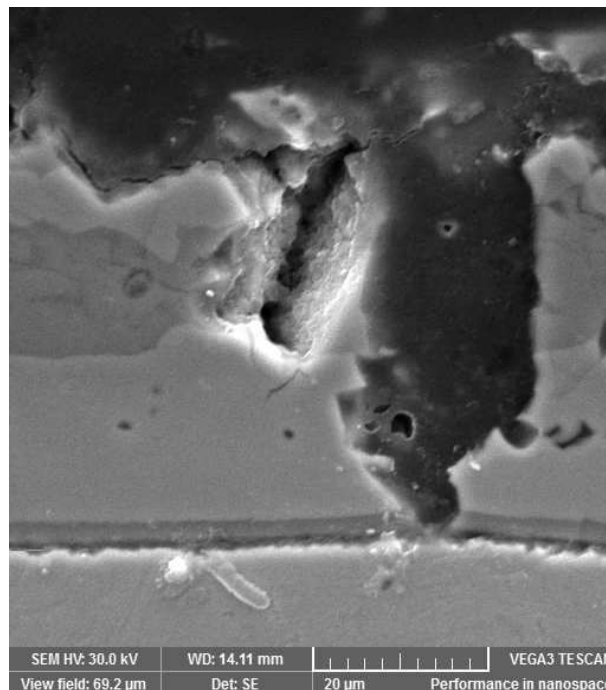


Fig. 10 Sample 3, interruption of the surface layer

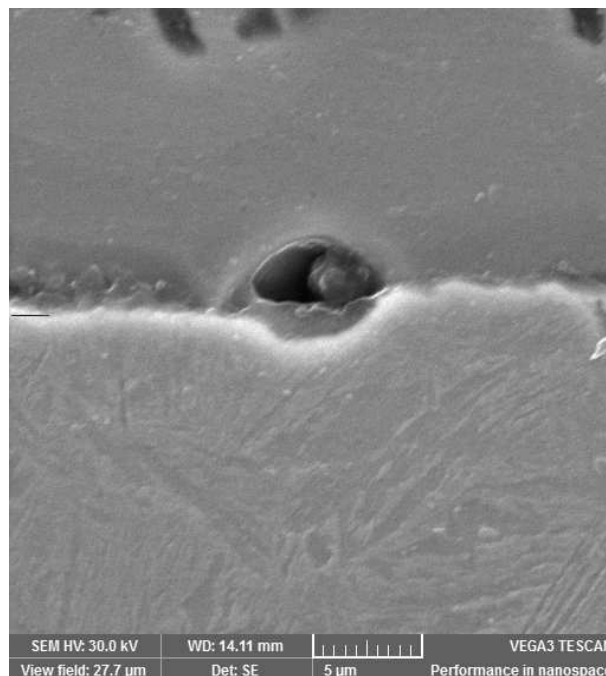


Fig. 11 Sample 3, inclusion in interlayer

In sample 3 (Figure 10), which was also investigated after forming of the blank, the observed areas were observed in the electron microscopy analysis, where the surface layer was interrupted locally, Fig. 10. Fig. 11 illustrates the interruption of the interface of the surface layer

with the base material and also documents the occurrence of particles in the interfacial interface. It can be presumed that this particle has not been removed during pre-treatment during application of the surface layer, it is already the above-described spherical inclusion.

Further investigation of the specimen was focused on the area of the base material (area 1) and the area around the particle in the interlayer (region 2) where EDX analyzes were performed, Fig. 12. Analytical values are shown in Tab. 4. The high Fe content is understandable, but also in all cases there is a high Mn content, which should according to the standards be only in an amount up to 1.4 wt.%. A high O content was recorded only for the particle in the interlayer and the area adjacent to it. In this area also increased Si content. It can be assumed that diffusion from the surface layer into the base material took place here.

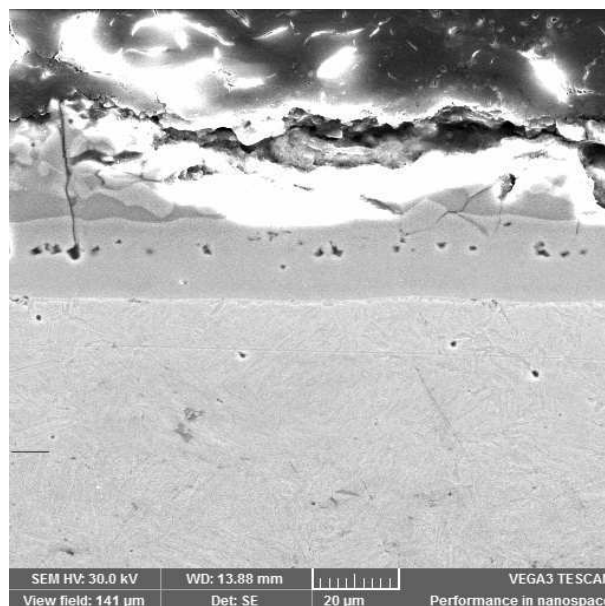


Fig. 12 Sample 3, cavities in the surface layer

Tab. 4 Area EDX analysis [wt. %]

Area	Fe	Mn	O	Al	Si	S	N	P	Mo	C	B
Area 1	78.66	18.58	0.09	0.00	0.00	0.00	0.00	0.00	0.00	0.51	1.97
Area 2	62.51	14.56	16.14	1.38	0.86	0.00	0.74	0.02	3.71	0.00	0.00

4 Discussion

The Olympus BX51M optical microscope, the TESCAN VEGA 3 scanning electron microscope, and the Brucker Esprit 2 analyzer were used to analyze the state of the Al-Si surface layer.

Macroscopic analysis was performed on both the blank and the molded part. On the molded part, the cohesion of the surface layer was interrupted. This interruption occurred mainly in places that were formed at the angle or in the areas of the unequal profile. From this it can be concluded that the surface layer defect was formed during the molding process.

The microscopic analysis was first performed from sites of surface Al-Si surface failure. Degradation of the surface layer was observed in these samples. Where there was a "galling", the incidence of globular inclusions was recorded. By conducting EDX analysis, a high content of Nb was found in spherical inclusions. It can be assumed that Nb was included in the carbide nitride forming tool used to increase the strength of the tool and that the molded surface was transferred during the molding process. In addition, macro cracks in the surface Al-Si layer were observed which occurred in almost all areas of the surface of the molded part. Their occurrence was periodically recurring and the macro cracks always had the same width. The formation of macro-cracks is related to the accuracy of the forming mold and its adjustment, in particular in the enlarged gap created when pressed forms of these macro-cracks due to the different thermal conductivity of the base material surface and the Al-Si layer.

The microscopic analysis of the blank showed an even thickness of the surface Al-Si layer, which is just above the upper limit of the specified thickness according to the

technical specifications of BS: EN 10346: 2009 for the surface layer. The thickness of the surface Al-Si layer was $(32 \div 35) \mu\text{m}$. It can be assumed that the higher thickness of the surface Al-Si layer has lower thermal conductivity, and therefore, macro-cracks are easier to produce in the thermal treatment.

Furthermore, a microscopic analysis of the molded part was performed, by which the uneven thickness of the surface Al-Si layer and the pores in this layer was found. The total thickness of the Al-Si surface layer is $(20 \div 30) \mu\text{m}$, thus it does not reach the required values according to the internal regulations. At the outer edge of the complex surface layer there are pores that originate according to sources with Kirkendall's effect. Kirkendall's effect in the case of this material is manifested by a higher diffusion coefficient of the surface Al-Si layer compared to the base material 22MnB5. It can be assumed, therefore, that the pores in the surface Al-Si layer reduce the cohesion of the various surface Al Si layers, which is reflected in the surface quality of the sheet metal.

5 Conclusion

The aim of the paper was to point out the possibility of using microscopy methods in the analysis of the behaviour of the surface Al-Si layer on steel sheet in the surface forming process. The 22MnB5 steel sheet with a surface Al-Si layer was used as the experimental material. The blank with the initial ferritic-pearlitic structure was heated in the oven above the austenitizing temperature. After being removed from the furnace, the part was molded to the desired shape and cooled on a martensitic structure. On the results based on analyzes carried out, it follows that:

- It is important to check the Al-Si layer and its

parameters for engineering practice. It is important to control the thickness of the surface layer in order to avoid problems with a higher thickness of the surface layer which leads to the cracking of this surface layer due to its thermal permeability and the formation of different stresses in the base material and the surface layer.

- In the base material of the work piece, it is necessary to check the prescribed input microstructure (ferritic-pearlite) and the material purity, which can influence the process of austenitization and subsequent heat treatment.
- Another factor that affects the quality of the resulting work piece is the quality of the forming mold (its surface condition, geometry and setting parameters). The mold has a significant effect on the formation of surface layer damage. In the event of galling on the surface of the mold, this form must be blocked and repaired. Thus, to prevent degradation processes of the surface protective layer Al-Si in the manufacturing process of bodywork.

Acknowledgement

Authors are grateful for the support of grant No. CZ.1.05/4.1.00/11.0260 EDIMARE and SGS FME JEPU in Ústí nad Labem for 2018.

References

- [1] Steel Types. [online] [cit. 2018-30-07]. Available from <http://www.worldautosteel.org/steel-basics/steel-types/>
- [2] PTÁČEK, L., (2002). *Material Science II*. CERM, Brno.
- [3] Deep Drawing. [online] [cit. 2018-30-07] Available from http://thelibraryofmanufacturing.com/deep_drawing.html
- [4] KOCICH, R. (2012). *Thermo mechanical forming processes*. p. 117. Ostrava.
- [5] SKRIKERUD, M., Press hardening from a global perspective. [online] [cit. 2018-30-07]. Available from https://www.oerlikon.com/ecomaXL/files/oerlikon_AP_T-presentation-Schopfheim-handout.pdf?download=1.
- [6] WINDMANN, M., RÖTTGER A., THEISEN W., (2014). Formation of intermetallic phases in Al-coated hot stamped 22MnB5 sheets in term soft rating thickness and Si content. In *Science Direct* [online], pp. 17-25.
- [7] WINDMANN, M., RÖTTGER A., KÜGLER H., THEISEN W., (2015). Removal of oxides and brittle coating constituents at the surface of coated hot-forming 22MnB5 steel for a laser welding process with aluminium alloys. In *Science Direct* [online]. pp. 153-160.
- [8] WANG, K. JIN, Y., ZHU, B. ZHANG, Y. (2016) Investigation on cracking characteristic of Al-Si coating on hot camping boron steel parts based on surface strain analysis. In. *Science Direct*, pp. 282-294.
- [9] DURICA, J., JURCI, P., PTACINOVA, J. (2018). Microstructural evaluation of tool steel Vanadis 6 after sub-zero treatment at -140 °C without tempering. In. *Manufacturing Technology*, 18 (2), pp. 222-226.
- [10] KUSMIERCZAK, S., NAPRSTKOVA, N. (2018). Comparison of semifinished product influence on surface degradation of forging rolls, *Engineering for Rural Development*, 17, pp. 1372-1377.
- [11] BORKO, K., PASTOREK, F., FINTOVA, S., NESLUSAN-JACKOVA, M., HADZIMA, B. (2017) Study of phosphate formation on S355J2 HSLA steel. In. *Manufacturing Technology*, 17 (1), pp. 8-14.